

Numerical Study of Heat Sink Models Mosquito Hotend on FDM 3D Printer to Determine Heat Transfer Characteristics

Rafi Fadhlorrohan^{1*}, Bambang Arip Dwiyanoro¹

¹Department of Mechanical Engineering, ITS, Sukolilo Surabaya 60111, Indonesia

Received: 12 January 2024, Revised: 15 February 2024, Accepted: 21 February 2024

Abstract

Fused Deposition Modelling 3D printing technology is generally used to print polymer-based materials in the form of filaments. The FDM process begins with the filament entering the liquefier area through the throat using a filament feed mechanism. During this process, clogging often occurs in hotend components because the filament melts before reaching the heat block. The clogging phenomenon will result in the filament being unable to extrude properly so the results are not optimal. In this research, a numerical study will be carried out to review the temperature distribution of the Mosquito hotend, as well as the effect of variations in air flow velocity at speeds of 0 m/s, 0.25 m/s, 0.5 m/s, 0.75 m/s, and 1 m/s. Based on the results of the CFD simulation, it was observed that the temperature at the Mosquito hotend is spread asymmetrically. On the heat sink component, the part facing the inlet of the airflow and the farthest point from the heater has a lower temperature than the opposite side. This causes an asymmetrical temperature distribution during the heat break so that the filament melting process does not occur evenly, which will result in clogging. In addition, airflow with a faster velocity will provide a better cooling system quality. This happens because the convection coefficient increases with the increase in air velocity, thereby increasing the amount of heat to be dissipated.

Keywords: 3D Printing, FDM, Mosquito Hotend, Heat Sink

1. Introduction

Fused deposition modeling (FDM) 3D printing technology is generally used for printing with polymer-based materials, such as Acrylonitrile-Butadiene-Styrene (ABS) and Polylactic Acid (PLA) in filament form [1]. The FDM process begins with the extrusion of filaments into the hotend component in solid form, when the filament temperature approaches room temperature (27°C), before approaching the glass transition temperature, which is around (55°C-60°C) for PLA [2]. The conditions that need to be considered in the hotend component of FDM 3D printers are the need to increase the temperature so that the filament melts in zone melting zone and keep the temperature as low as possible to keep the filament in solid condition in the cold zone. Therefore, an optimal mechanism is needed to support these temperature parameter conditions.

Shukla et al. [3] conducted research a numerical study on the components of the liquefier and observed the heat distribution. The phenomenon of heat distribution is observed when the heating element is heated at 215°C. Based on the test results, the temperature distribution in the liquefier is longitudinally asymmetric. This occurs due to uneven heating with heating occurring more dominantly on one side of the liquefier than the other. This phenomenon results in non-uniform and inhomogeneous

polymer melting and solidification.

Hofsetter Jr. [4] explained the phenomenon of heat creep in FDM-type printers. In the process of heating the nozzle to reach a certain temperature, heat will move from the heating element to the metal components on the hotend. When the filament is pushed toward the nozzle, the heating wall on the printer head softens the filament so that the filament will collect in the space in the nozzle components before exiting to the end of the nozzle. The addition of a cooling fan as a forced convection component to provide airflow around the heat sink can help dissipate heat properly.

Muthusami & Zarbakhsh [5] research the effect of fin size on heat sinks on temperature distribution and clogging zone settings in extrusion-type 3D printers. Based on the study results, the fin size should not exceed 20 mm as the most efficient design compared to other sizes. If the fin size exceeds 20 mm, then the heat sink will experience over-engineering because there is no change in the size of zone 2 for fin sizes above 20 mm. This result only applies to the melting temperature of the filament material of 260°C.

Kumar et al. [6] does a numerical study to analyze the thermal phenomenon of the heat sink with the Rep-Rap 3D Printer Liquefier. This research was conducted by simulating the CFD model using ANSYS Fluent. Based on

*Corresponding author. Email: rafifadhlorrohan1@gmail.com
© 2024. The Authors. Published by LPPM ITS.

the simulation results, it can be observed that the temperature of the heat sink using circular fins is lower when compared to heat sinks using rectangular fins. It can also be observed that the surface temperature of the heat sink decreases as the airflow velocity increases. The conclusion from this study is that heat sinks that use circular fins with variations in airflow velocity have better heat transfer rates due to the increased surface area of the heat sink.

One of the FDM 3D printer component manufacturers, Slice Engineering, produces what is now one of the best hotend, the Mosquito hotend. However, based on experiments conducted, this hotend still has weaknesses, where there are still problems with clogging that result in poor printing quality. This happens due to the heat creep phenomenon still occurring in the hotend component. The object that is observed is one of recently the most recommended hotend because of its reliability to work for long hours and high temperatures. As an initial hypothesis, the cause of heat creep and clogging is due to poor cooling quality in the Mosquito hotend. By observing the heat transfer characteristics in the heat sink component using simulation methods using Ansys Fluent, it is hoped that the cause of heat creep and its solutions can be found. This research combined methodology and analysis from previous research. It uses the CFD method to simulate the working conditions and analyze the temperature distribution. There may be some possible limitations in this study, where a numerical approach to actual working conditions

still becomes a challenge. Filament that flows along the hotend and phase change of the filaments are still not applied to this research.

2. Numerical method

2.1. Development of Object Models

The Mosquito hotend design is provided by Slice Engineering Manufacturing which can be accessed from the company website. Data specification about physical objects is provided in Table 1. The following is the model along with the dimensions of the object. Details of the object dimensions can be observed in Figure 1.

2.2. Numerical Data Processing

The input geometry is in accordance with Figure 2, but then the model will be simplified to make it easier at a later stage. Mosquito hotend components consist of 3 parts, namely heat sink, heat break, and heat block. Then, there is also a fluid domain as the surrounding air. In numerical simulation, meshing is used to divide the simulation area into smaller elements, and then calculate and place these elements to get more accurate results, which can be seen in Figure 3.

As the inlet at the domain entrance, the velocity inlet is defined with constant velocity based on variations. The exit is defined as pressure outlet boundary conditions. The heat source of the hotend is placed at the heating element and defined as a wall with constant surface temperature.

Table 1. Mosquito hotend specifications

Manufacturer	Slice Engineering
Dimension	19 x 25 x 41 mm
Working temperature	0°C - 450°C
Heat sink (Cooling Tower)	Aircraft-Grade Aluminium (Alloy 7075)
Heat break	Bimetallic: Copper Alloy & Strained Stainless Steel
Heat block	High-Grade Copper Alloy

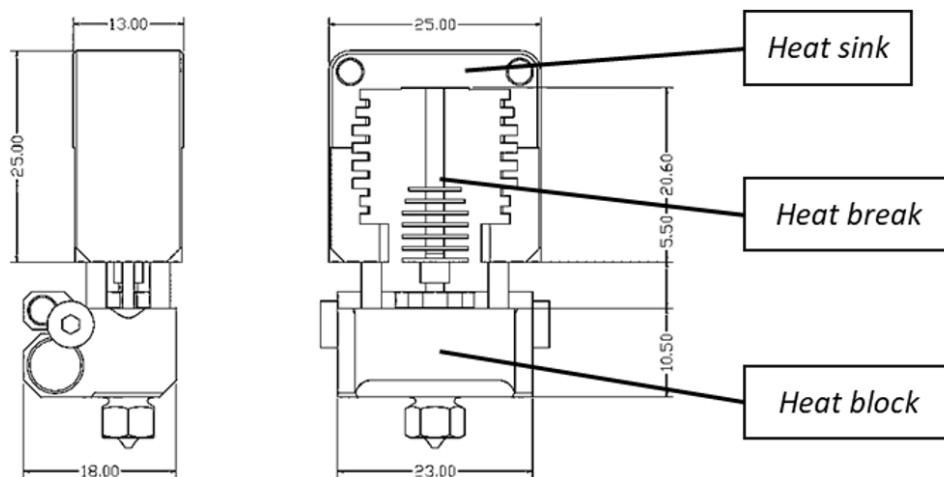


Figure 1. Sketch and dimension of Mosquito hotend

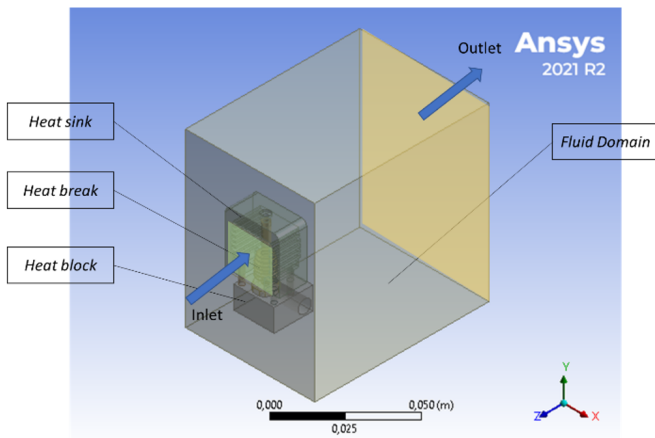


Figure 2. Model geometry and fluid domain

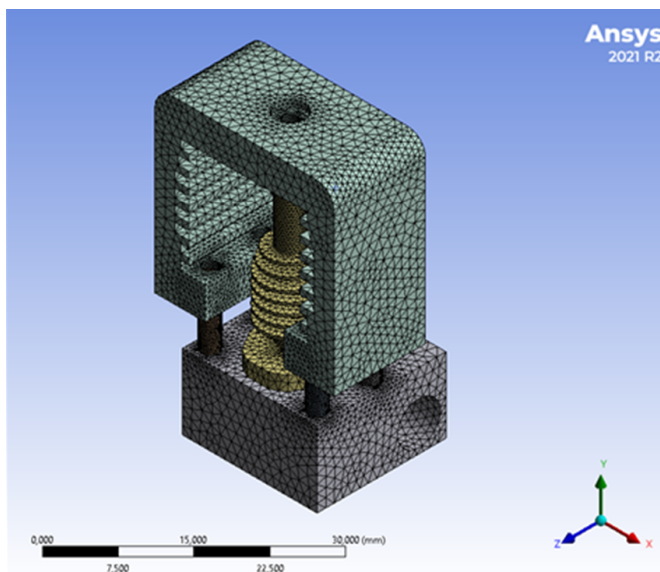


Figure 3. Object mesh that will be simulated

a) Numerical Method

The simulation condition is in a steady state. For turbulence models, RNG $k-\epsilon$ is used. SIMPLE is used as Pressure-Velocity coupling. Also, second-order discretization is used as a solution method [7, 8]. In this study, to determine the effect of variations in inlet airflow velocity on the temperature profile of the heat sink, speed variations are 0, 0.25, 0.5, 0.75, and 1 m/s were carried out by running the geometry and meshing that had been formed and achieving grid independence in ANSYS software based on operating conditions and repeating them using the specified speed variations.

b) Post-processing

The output of this variation is a comparison temperature profile graph of each inlet speed vari-

ation. The graph presented is the relationship between the temperature on the upper face of the heat sink and the air velocity due to the fan. In this graph, there is a temperature profile at each review point on the wall with different speed variations. In addition, from this speed variation, a graph of the relationship between inlet speed and heat loss is also obtained.

3. Results and Discussion

3.1. Grid Independency Test

In this study, a grid independency test was conducted, by conducting simulations based on parameters and solving according to the research method, using an airflow velocity of 1 m/s. Then, the output parameter observed is the minimum temperature at the top heat sink. Then the relative error value is calculated to compare between mesh element sizes.

Based on Table 2, it can be observed that the minimum temperature value at the top heat sink tends to fluctuate along with the smaller element size. Then, the relative error is calculated with the smallest value and the convergent result is at a mesh element size of 1.2 mm. By considering the accuracy of the results and the duration of the calculation, the mesh element size that will be used is 1.2 mm.

Table 2. Grid independency test results

Mesh Element Size [mm]	Mesh Elements	Top Heat Sink Minimum Temperature (°C)	Rel. Error
2	631,564	111.48	
1.5	741,776	113.00	1.34%
1.2	990,683	112.80	0.17%
1	1,348,626	112.10	0.62%
0.9	1,652,938	111.35	0.68%

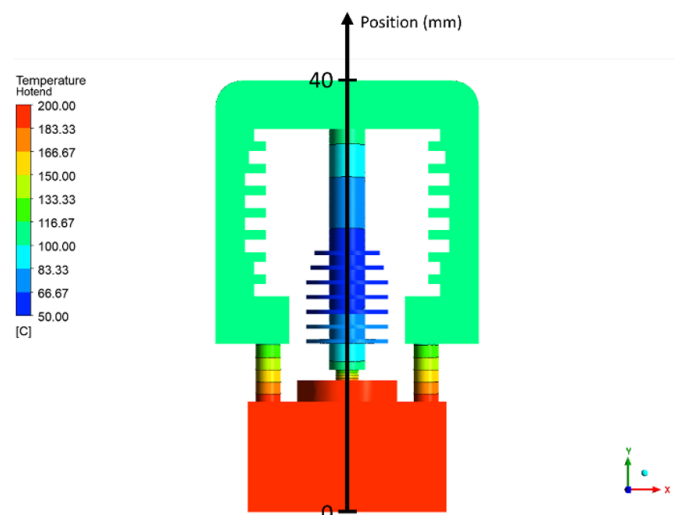


Figure 4. Temperature distribution contour of Mosquito hotend

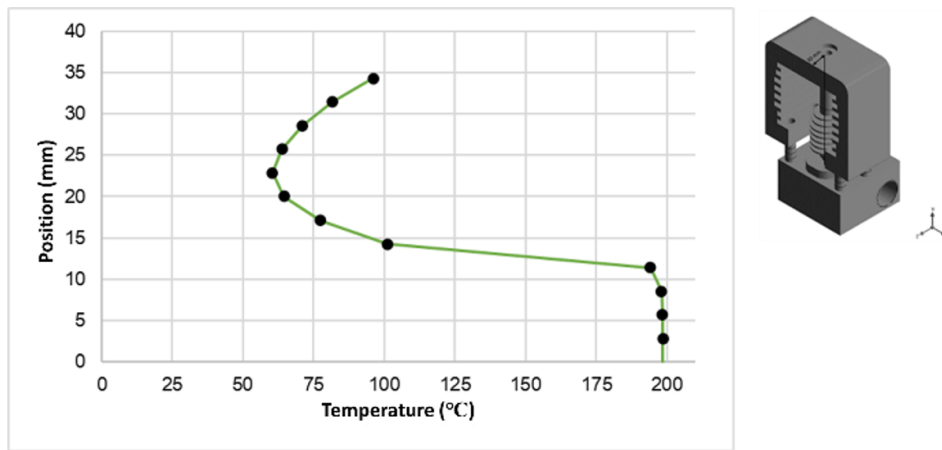


Figure 5. Temperature distribution of Mosquito hotend

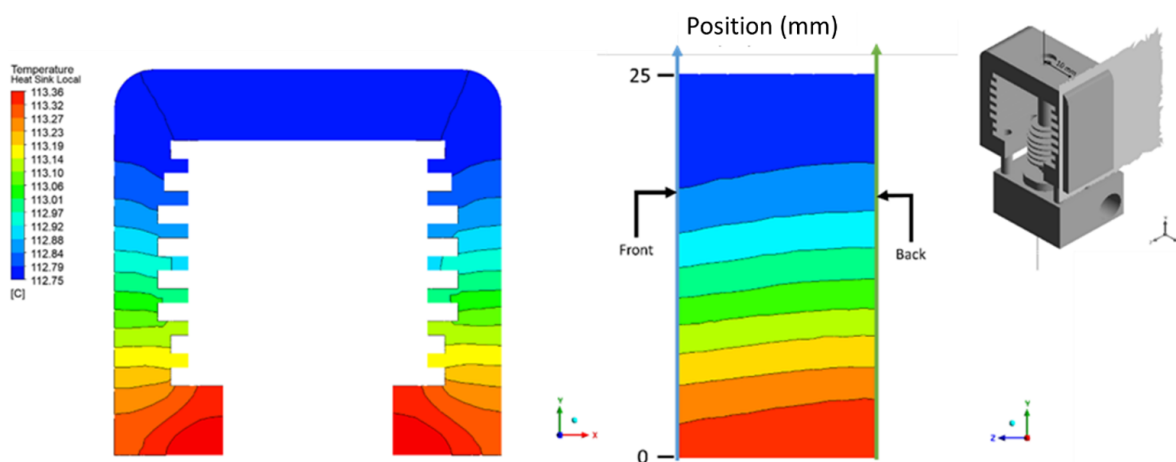


Figure 6. Temperature distribution contour of heat sink component

3.2. Analysis of Mosquito Hotend

a) Temperature Distribution of Mosquito hotend

The temperature distribution on the Mosquito hotend can be observed in Figure 4, the highest temperature is 200°C on the heat block component and the lowest temperature is 50°C on the heat break component. Heating from the heater on the heat block component propagates from the heat block which has a high temperature to the standoff and heat break components. Then, the heat propagates from the standoff to the heat sink.

Based on Figure 5, it can be observed that the temperature distribution fluctuations at the hotend are not inversely proportional to the overall distance from the heater. This is because the heating generated from the heat block makes the temperature from the bottom of the heat break increase, then gradually decrease because the center of the heat break is passed by a velocity airflow that helps in dissipating the heat in the heat break. Then, the higher up, the temperature will increase again. This is the

effect of the heat sink which helps to dissipate heat. However, due to the influence of the heat sink which has not dissipated heat properly, the temperature at the top of the heat break increases.

The effect of this phenomenon will make the filament experience an additional zone, namely pre-heating. The increase in temperature until it reaches the glass transition temperature (55 °C - 60 °C) will make the filament begin to change its form to semi-liquid. The changes in loading and position that occur during the extrusion process will put the filament in a temperature-optimal condition.

b) Temperature Distribution of Heat Sink

Based on the temperature contours in Figure 6, it can be seen that the temperature distribution on the heat sink is high at the bottom, then decreases vertically to the top. This happens because the heat from the standoff moves to the heat sink through the bottom of the heat sink. In addition, it can also be observed in the side view, that the temperature tendency is higher on the right side horizontally (behind the heat sink).

The scheme of the phenomenon that occurs in the heat sink can be observed in Figure 7, where the horizontal temperature distribution is not symmetrical on the heat sink component, where the temperature in the front heat sink facing the airflow is lower than in the back heat sink. This happens because the high temperature of the heat block flowing into the standoff is not centered in the middle, so there is a tendency for one side to have a higher temperature. In addition, the direction of airflow facing one side of the heat sink, resulting around the heat sink closer to the direction of air entry occurs better heat dissipation than those closer to the direction of air exit.

c) Temperature Distribution of Heat Break

Observations on the heat break component were made by looking at the temperature contours in the center of the heat break as shown in Figure 8. The temperature on the heat break is highest up to 200°C at the bottom of the heat break which is in direct contact with the heat block component as a heat source. Then, the higher the temperature decreases to a temperature of 55°C but again increases upwards to a temperature of 117°C.

The Mosquito hotend design that separates the heat break and heat sink components creates temperature distribution characteristics that are different from the hotend design in general. The temperature on the heat break vertically decreases in the middle and increases again at the top.

d) Temperature Distribution of Heat Block

From the simulation results, plotting is done on the heat block by looking at the temperature contour at the intersection of the center of the heat block as shown in Figure 9. The temperature on the heat block is highest up to 200°C around the heater and has a temperature drop at the left end of the

heat block, with a temperature difference of about 4°C.

In Figure 10, the temperature distribution at the top of the heat block can be observed. Based on the heat transfer propagation that occurs, the point that is further away from the heat source has a lower temperature. The largest temperature difference on the heat block is around 4°C. This is similar to the results of research by Shukla et. al, where the heat block component has a temperature difference of 3.5 degrees Celsius. Heat transfer on the heat block from the heater which is set at 200°C. The propagation occurs in all directions, but due to the position of the heater which is not in the center resulting in the spread of temperature distribution is not symmetrical. The effect of asymmetrical heat distribution will affect the performance of the hotend where the heat will be distributed unevenly in each component vertically.

3.3. Analysis of Air Flow Velocity Variations Passing Through the Mosquito Hotend

Based on observations in Figure 11, the effect of airflow velocity can be analyzed that the increasing speed of airflow passing through the hotend component will provide a lower temperature. This is similar to the results of research by Kumar, Verma, & Nagpure in 2017, namely the higher the airflow velocity, the better the heat transfer rate. Providing airflow in the hotend area will help in the convection heat dissipation process. The quality of convection will be better if the airflow velocity is faster. After simulating the speed variation on the Mosquito hotend, the temperature contour scheme can be observed in Figure 12. The variation of airflow speed results in the lowest temperature experienced at the heat break will be lower directly proportional to the airflow speed.

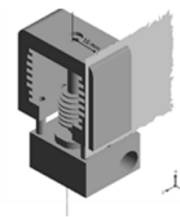
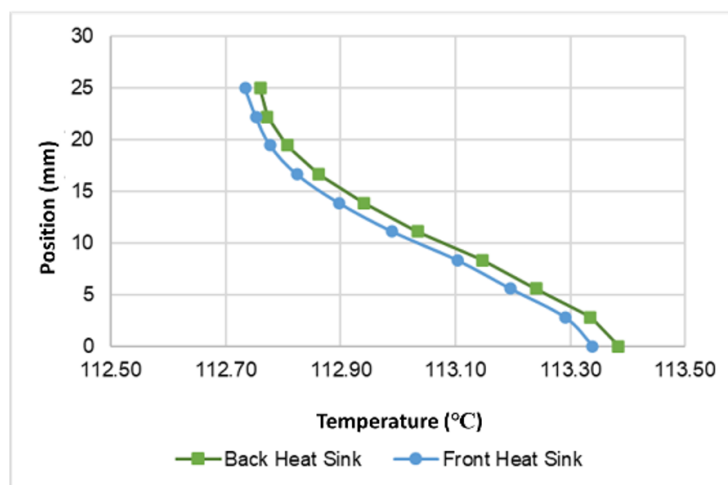


Figure 7. Temperature distribution of heat sink

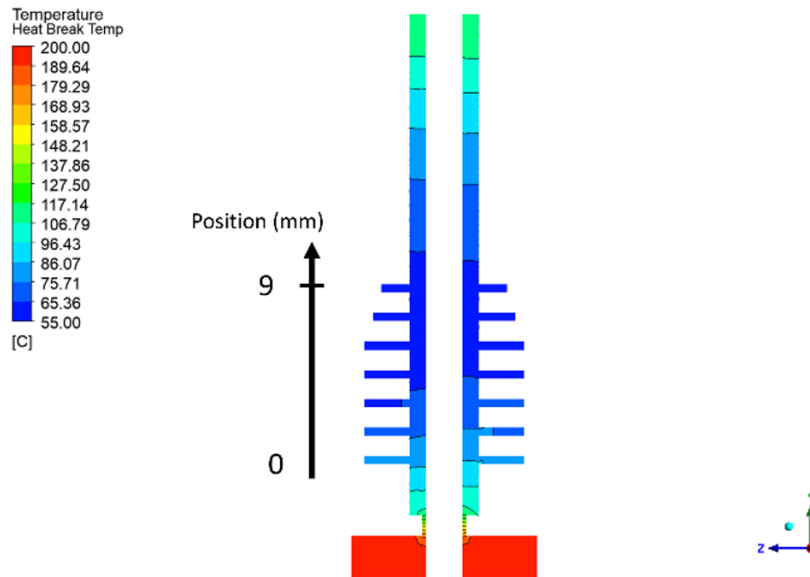


Figure 8. Temperature distribution contour of heat break

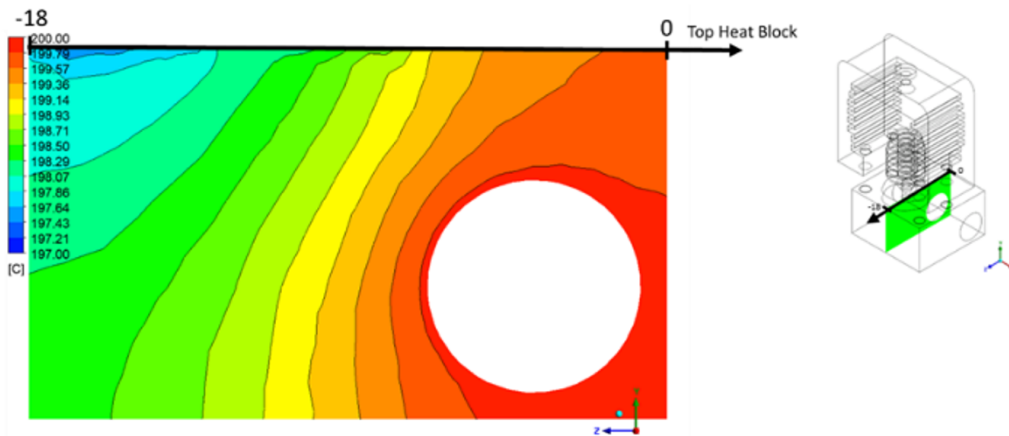


Figure 9. Temperature distribution contour of heat block

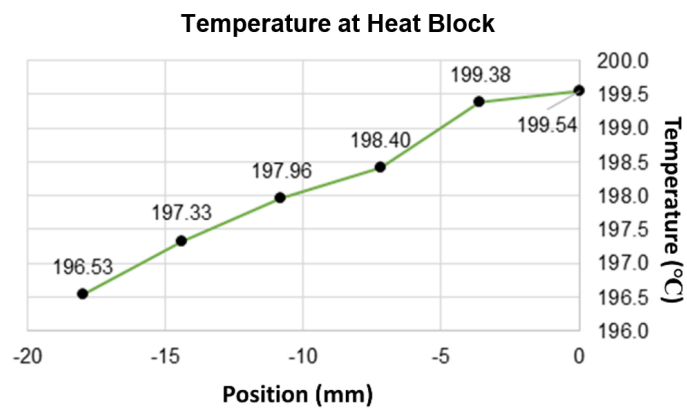


Figure 10. Temperature distribution at top of heat block

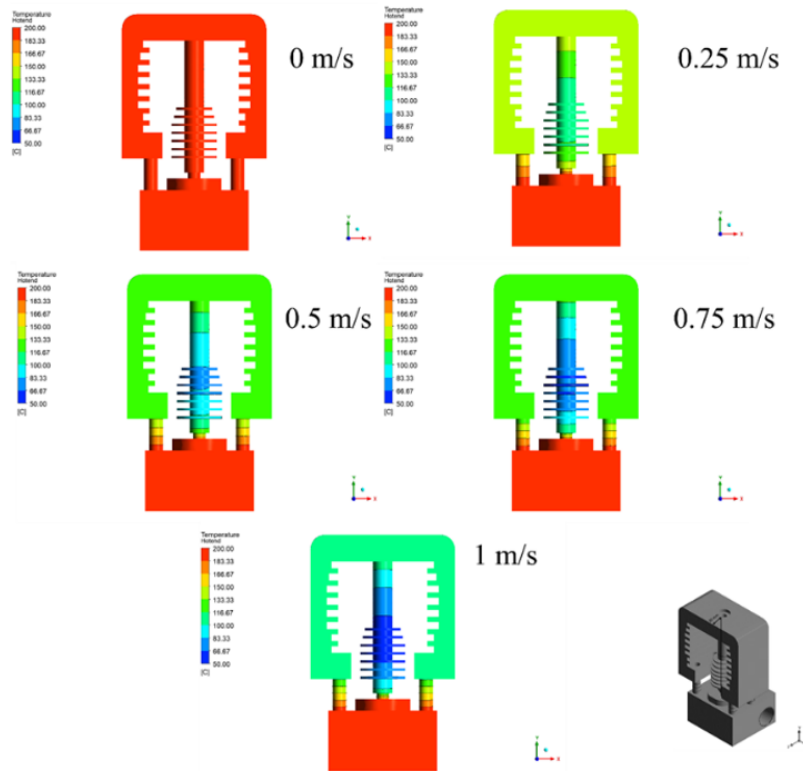


Figure 11. Temperature distribution contour of Mosquito hotend with air velocity variations

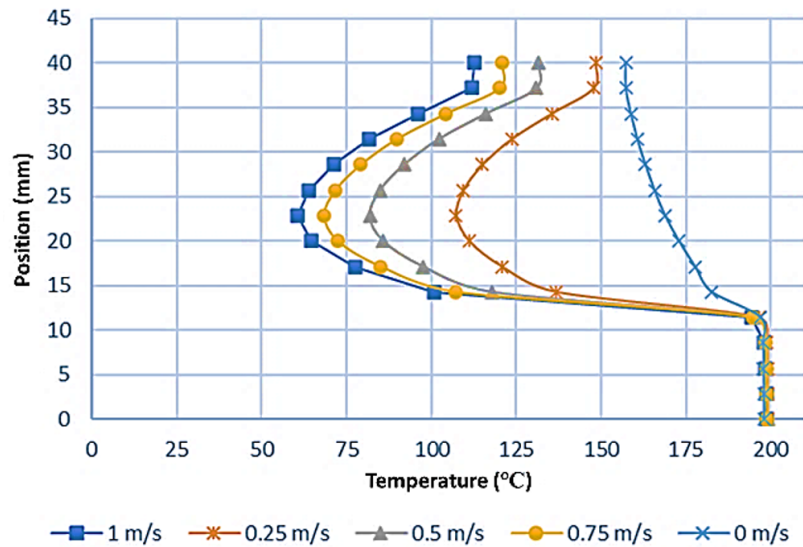


Figure 12. Temperature distribution at the center of Mosquito hotend with air velocity variations

The speed variation that has the area at the heat break with the lowest temperature is the air speed of 1 m/s. In addition, the area that experiences a transition zone under the glass transition temperature, namely at a speed of 1 m/s. However, at speeds of 0.5 m/s and 0.75 m/s, the Mosquito hotend has experienced glass transition temperature although not so well. This can also be observed based on the temperature distribution graph in Figure 12.

The area that has low temperature on the hotend shows the transition zone area. As the airflow speed gets faster, the area with low temperature will be wider. This shows that to get a narrow transition zone, it needs to be adjusted based on the glass transition temperature of the filament and the airflow velocity to get an ideal transition zone. The results and discussion can be presented in one section or separate sections and can be divided into sub-sections.

4. Conclusions

Based on the description contained in the results and discussion above, the following conclusions can be obtained.

1. Temperature distribution on the Mosquito hotend is spread asymmetrically. This is due to the position of the heater on the heat block which is located on the part that leads to one side, so that the heat propagation to each heat sink component is uneven. In addition, the direction of airflow entry at the front of the heat sink results in maximum heat dissipation

on the front side of the heat sink. Asymmetrical temperatures will cause filament melting to occur irregularly which will result in clogging.

2. Based on the simulation results, the flow velocity with the best cooling system quality is 1 m/s. The greater the air velocity passing through the Mosquito hotend, the lower the temperature distribution.

Acknowledgments

The authors have stated that there is no conflict of interest.

References

- [1] J. Jafferson and D. Chatterjee, "A review on polymeric materials in additive manufacturing," *Materials Today: Proceedings*, vol. 46, pp. 1349–1365, 2021.
- [2] V. Shanmugam, O. Das, K. Babu, U. Marimuthu, A. Veerasimman, D. J. Johnson, R. E. Neisiany, M. S. Hedenqvist, S. Ramakrishna, and F. Berto, "Fatigue behaviour of fdm-3d printed polymers, polymeric composites and architected cellular materials," *International Journal of Fatigue*, vol. 143, p. 106007, 2021.
- [3] V. V. Shukla, A. K. Kulkarni, A. K. Pingle, and S. Oza, "Thermal analysis of 3-d printer liquefier indicates a probable cause of nozzle clogging," *Int. J. Mech. Prod. Eng. Res. Dev.*, vol. 9, no. 2249-8001, pp. 176–182, 2019.
- [4] D. D. J. Hofstetter, "Understanding the lulzbot taz 5 3-d printer and dual extruder v3 print head," *Bennett Aerospace, Inc.*, 2021.
- [5] A. Muthusami and J. Zarbakhsh, "Effect of heat sink fin size on temperature distribution and control of clogging zone in 3d printer extruders,"
- [6] M. K. P. K. S. Verma and S. Nagpure, "Numerical simulation of rep-rap 3d printer liquefier to determine the thermal behavior of heat sink," 2017.
- [7] R. P. S. W. Galih and B. A. Dwiyantoro, "Effect of diffusers installation in inlet primary air coal pulverizer on airflow characteristic and wear concentration using cfd modeling," *JMES The International Journal of Mechanical Engineering and Sciences*, vol. 6, no. 2, pp. 57–74, 2022.
- [8] B. A. Dwiyantoro and S.-W. Chau, "The dependence of microdroplet size on the parameters governing the dewetting process on circular micropillar arrays," *Journal of Mechanical Science and Technology*, vol. 27, pp. 2005–2013, 2013.